Civil Engineering Beyond Limits 3 (2025) 11005
Civil Engineering Beyond Limits
journal home: www.acapublishing.com/journals/1/cebel

Research Article

Behavior of Plastic-Geogrid Reinforced Asphalt Concrete

Saad Issa Sarsam*,[1]
[1]Professor, Sarsam and Associates Consult Bureau (SACB), Baghdad-IRAQ. Former Head, Department of Civil Engineering, College of Engineering, University of Baghdad, Iraq.

Keywords

Geogrid,
Asphalt concrete, Viscoelastic behavior, Reinforcement,
Stiffness,
Load bearing capacity, Interlayer.

Abstract

Grid reinforced overlays are considered for flexible pavement rehabilitation to ensure that the pavement condition can be maintained, with extended service life. This work evaluates the influence of two types of plastic biaxial geogrid reinforcement (AR-G and AR-1) on viscoelastic behavior of asphalt concrete in terms of stiffness, deformation, and load bearing ability. Asphalt concrete mixture for surface course layer was prepared. Circular asphalt concrete specimens of 152 mm diameter and 38 mm thickness have been constructed with optimum asphalt content, and static compaction to a target density. The overlay mixture was compacted over those circular specimens, and the Grid reinforcements were introduced in between, then, tested in a model box of 50 x50 x70 cm filled with loose sand layer of 40 cm thickness representing the existing subgrade. It was found that at failure, the load bearing capacity increased by (56.25 and 55.62) % for grid reinforced mixture with (AR-1 and AR-G) respectively as compared with the control mixture. Smaller aperture size and lower thickness of geogrid had furnished higher load bearing capacity for AR-1 geogrid as compared with that of AR-G geogrid. The stiffness of the grid reinforced asphalt concrete is higher than that of the control mixture by (56.2, and 62.5) % for AR-G and AR-1 geogrids respectively. It was concluded that implementation of the geogrids is beneficial in enhancing the sustainability of asphalt concrete. The obtained mathematical models of viscoelastic and viscoplastic failure stages can be used to predict the improvement in the properties of reinforced asphalt concrete.

1. Introduction

The contribution of geogrid significantly can add to extending serviceability of the flexible pavement and improving benefit/cost analysis. Geogrids in asphalt overlays are expected to develop a type of reinforcement mechanisms that contribute to the pavement structural capacity and may improve the mechanical behavior of the flexible pavement by controlling permanent deformation and reducing strains in the pavement layers. Zofka et al., 2017 [1] investigated the effect of geogrid reinforcement on asphalt concrete specimens under mono tonic and cyclic testing. A significant strengthening contribution of geogrid was observed regarding the fracture and deflections of the mixture. A reduction of pavement deflections due to the geogrid application a significant extension of pavement fatigue life was observed. Brusa et al. 2016 [2] presented a design methodology which is an empirical mechanistic process for reinforced asphalt concrete pavement. Geogrid Reinforcement design software of Asphalt Pavements was presented and recommended for use in overlay design. Zofka et al., 2017 [3] assessed the benefits of using geogrids within asphalt concrete pavement layers. Glass and carbon geogrids were implemented as reinforcements. Specimens were evaluated to observe their behavior under stress-controlled fatigue test and strain-controlled fracture test. Results demonstrated a beneficial and positive influence of reinforcement. Correia1 and Zornberg, 2016 [4] presents the results of large model tests involving polyvinyl alcohol geogrid as reinforcement and unreinforced hot mix asphalt overlays. Cyclic wheel loads were applied. A considerable increase in pavements structural performance was noticed. The use of geogrid as reinforcements was found to reduce permanent lateral movements in the surface layer. It was concluded that geogrids can provide enhanced structural capacity to flexible pavements. Correia1 and Zornberg, 2018 [5] investigated the distribution of tensile strains along geogrids used to reinforce asphaltic layers. The permanent and elastic displacements induced in geogrids were examined with the aid of strain gages. It was observed that elastic tensile strains in the asphalt mixture and rutting under the wheel path were comparatively smaller when using geogrids as compared to the case of unreinforced asphalt concrete. It was concluded that implementation of geogrids in asphalt concrete overlays exhibits lateral restraining mechanism which had an influence on the mechanical behavior of flexible pavements. Lee et al., 2022 [6] analyzed the advantages of carbon grid reinforcement in asphalt pavement based on performance tests with the aid of four-point bending, and shear bond strength test. It was detected that carbon grid reinforcement can enhance the performance of asphalt mixture and prolongs service life of the flexible pavement. The resistance to reflection cracking was improved while the rutting velocity was reduced due to the presence of a grid layer. Orešković et al., 2024 [7] proposed a new approach to calculate the number of cycles to failure during the four-point bending beam fatigue tests of control and grid reinforced asphalt concrete. The impact of reinforcement on fatigue life was evaluated by comparing the critical strain values of reinforced and unreinforced sets through fatigue resistance. It was revealed that the use of geogrids improves fatigue life, and that the traditional approach of (50% reduction in initial stiffness is considered as failure criterion) might not always be appropriate for assessing the fatigue resistance of reinforced asphalt mixtures. Alimohammadi et al., 2021 [8] reveals that improvement of the asphalt concrete performance due to the grid reinforcement is related to geogrid geometry and stiffness, geogrid depth, asphalt layer thicknesses, and subgrade stiffness. Realizing and understanding the structural benefits of geogrids can reduce the thickness of the asphalt pavement and extend the service life and reduce maintenance costs. Moreover, it is expected that the appropriate use of geogrids can be significantly saving per project. Mounes et al., 2016 [9] performed dynamic creep test on

*Corresponding Author: saadisasarsam@coeng.uobaghdad.edu.iq
Received 23 May 2025; Revised 10 Jun 2025; Accepted 10 Jun 2025
https://doi.org/10.36937/cebel.2025.11005

fiberglass grid reinforced asphalt concrete samples. The grids used contained different sizes of grid openings and tensile strengths. The results proved that grid tensile strength and grid mesh size are of great importance in resisting the development of permanent deformation. Higher tensile strength and smaller mesh size grids lead to better performance of grid reinforced samples. Correia and Mugayar, 2021 [10] investigated the effect of geogrid properties on the interface shear bond performance. It was reported that Geogrid physical characteristics exhibit more significant influence than geogrid tensile properties. The stiffer geogrid provided lower shear strength at the interface and lower shear stiffness. Ziegler, 2017 [11] stated that construction of geogrid reinforced flexible pavement exhibited significant advantages in terms of ecological and economic aspects against classical pavement. It is also well known that grid reinforced pavements have a much higher bearing capacity while the deformations are much lower than expected. Zarei et al., 2025 [12] evaluated the influence of implementing geogrids within the asphalt concrete layer on controlling rutting and cracking. Viscoelastic analyses of control and reinforced pavements were conducted using a three-dimensional finite-element model. The results indicate that placing high modulus geogrids can significantly enhance the pavement performance. Geogrid reinforcement, reduced shear strain by 48.4 % and vertical compressive strain by 28.1 % at 50 °C, which can control the rutting. Solatiyan et al., 2021 [13] revealed that implementing grid reinforcement at the interface of asphalt concrete layers, with varying degree of surface texture can significantly enhance the fracture toughness of the flexible pavement system, it exhibits combined functions of crack resistance and bonding quality. Liu et al., 2024 [14] investigated the performance of control and glass fiber geogrid-reinforced asphalt concrete pavement. A void was developed in the subgrade. It was found that the inclusion of geogrids extended the fatigue life of asphalt pavement. It was found that the inclusion of geogrid in asphalt had a limited effect on the dissipated energy in the pavements, and the composite module of the pavements increased. Chango et al., 2022 [15] investigated the influence of asphalt concrete material in the geogrid-reinforced-pile-supported embankment structure subjected to high-speed train moving. The asphalt concrete viscoelasticity behavior was incorporated into the geogrid-reinforced-pile-supported embankment model. The impact of asphalt concrete material characteristics was investigated, analyzed and discussed. Nguyen et al., 2024 [16] examined the performance of flexible pavement, considering geogrid's axial stiffness, geogrid's position within the pavement layers, and applied stress. It was found that the stress- strain response of the reinforced pavement was linear for the dynamic applied stress and nonlinear under the static applied stress, while the position of the geogrid has a significant influence on the pavement performance. Sarsam, 2013 [17] investigated the properties of biaxial geogrid reinforced asphalt concrete. It was revealed that thicker geogrids ribs exhibit better reinforcing performance when compared with thinner rip thickness of the grid. Andrea et al., 2014 [18] constructed an instrumented pavement section, glass fiber polymer grid and carbon fiber grid were installed inside asphalt concrete surfacing along an in-service road. It was concluded that the strain field inside the surface layer was considerably reduced after installation of the grid. Ragni et al., 2020 [19] assessed the possibility of rehabilitation of asphalt pavement with geocomposite to control rutting and cracking. Two types of beam specimen (unreinforced and reinforced with geocomposite) were obtained and tested for three-point bending tests. It was concluded that implementation of the geocomposite is an effective method to enhance asphalt pavement performance. Kumar and Jallu, 2022 [20] explored the efficiency of implication of the geogrids sandwiched between the bituminous layers subjected to interfacial shear properties. Therefore, the mechanical and flexural fatigue properties of geogrids embedded with asphalt layers were assessed and the effect of deformation, cracking, and service life of flexible pavements were monitored. Bekheet et al., 2019 [21] investigated the effectiveness of varying the geogrid type on the behavior of asphalt pavement. Two types of geogrids were used, Triaxial geogrid and Biaxial geogrid. Three-point bending beam tests were performed on beam specimens composed of two asphaltic layers, a surface course layer of 5 cm thickness and a binder course layer. The maximum loads and deformations were monitored. Test results indicate that implementing triaxial geogrid in asphalt concrete layers exhibits lower deformation and maximum load sustaining capacity. Leiva-Padilla et al., 2016 [22] measured and modelled the characteristics of asphalt concrete with a geogrid interlayer system prior to overlaying. The viscoelasticity properties were evaluated from Indirect Traction Tests. The increase in fatigue life, reduction in the cracking process when geotextile materials are used as interlayer system could be detected. Alimohammadi et al., 2021 [23] assessed geogrids' reinforcement effects on asphalt concrete. Cyclic load tests were performed to simulate vehicle-loading conditions. The test g results exhibited the positive effect of geogrid reinforcement in the structural performance of asphalt concrete pavements. It was stated that Biaxial and Triaxial geogrids caused a reduction in permanent deformation of (47 and 68) % respectively. Canestrari, et al., 2018 [24] stated that the service life of flexible pavements can be extended by installing geosynthetic reinforcements. Geogrids can be placed at the interface of asphalt concrete layers rehabilitating existing pavements, to improve rutting resistance and to delay reflective cracking. However, the geogrid inter-layer reinforcement supports the transmission of horizontal shear stress between asphalt layers.

The aim of the present assessment is to detect the influence of implementing two types of geogrids (AR-1 and AR-G) as inter-layers on the viscoelastic properties of asphalt concrete. The overlay mixture will be compacted over a prepared circular specimens of asphalt concrete after inserting the geogrids in between. Specimens will be tested under static load bearing test in a model box filled with loose sand which represents the poor subgrade. The load carrying capacity, deformation, and the stiffness of the control and grid-reinforced asphalt concrete specimens will be studied and compared through the unique testing setup for the experimental program.

2. Materials and Methods

2.1. Aggregates

Combiner coarse and fine aggregates were obtained from Al-Nubai, Mineral filler with 95 % finer than 75 micron was obtained from Karbala quarry; the physical properties are illustrated in Table 1. The testing was conducted as per the ASTM, 2015 [25] procedure.

Table 1. Physical properties of aggregates according to ASTM, 2015 [25] testing procedures

Property	Coarse aggregate	Fine aggregate	Mineral filler	ASTM Designation
Specific gravity	2.680	2.620	2.640	ASTM C-127 and C-128
Absorption (%)	0.4	0.7	Not applicable	ASTM C-127 and C-128
Percent Wear (Los-Angeles Abrasion)	19.6	Not applicable	Not applicable	ASTM C-131

2.2. Asphalt cement binder

Asphalt cement binder of penetration grade (40-50) was obtained from Dorah refinery; the properties are as illustrated in Table 2. The testing was conducted as per the ASTM, 2015 [25] procedure.

Table 2. Properties of Asphalt cement according to ASTM, 2015 [25] testing procedures

Property	Test results	ASTM Designation
Penetration (0. 1 mm)	48	ASTM D-5
Softening point (˚C)	49	ASTM D-36
Ductility (cm)	+100	ASTM D-113
Specific gravity	1.024	ASTM D-70

2.3. Geogrids

Two types of Tensar biaxial geogrids have been implemented; Table 3 illustrates their properties.

Table 3. Tensar biaxial geogrids reinforcement's properties (as supplied by the manufacturers)

Type of geogrid	Biaxial AR-G	Biaxial AR-1
Unit weight	0.25 gm./ m^2	0.24 gm./ m^2
Transverse strength	20 kN/ m	18 kN/ m
Longitudinal strength	17 kN/ m	14 kN/ m
Thickness	1.2 mm	0.8 mm
Aperture size	60x76 mm	51x71 mm
Polymer	Polypropylene	Polypropylene

2.4. Preparation of asphalt concrete mixture

Coarse and fine aggregates were mixed with mineral filler, the combined aggregates fall within the lower and upper limits of the SCRB, 2003 [26] specifications for wearing course pavement layer. The combined aggregates were heated to 160 ◦C then the required amount of asphalt cement binder which was heated to 150 ◦C was added and mixed thoroughly to create homogeneous asphalt concrete using mechanical mixer for 120 seconds. Table 4 presents the properties of the design asphalt concrete implemented. Figure 1 exhibits the combined aggregates gradation. The maximum size of aggregate was 19.5 mm, and the nominal maximum size was 12.5 mm which was implemented for the mix design. The mixing temperature was maintained to 160 ˚C.

Table 4. Properties of the Asphalt concrete wearing course mixture

Properties of asphalt concrete mixture	Test results	ASTM Designation
Optimum asphalt binder content (%)	4.8	ASTM-D-2172
Maximum theoretical specific gravity (Gmax)	2.482	ASTM D-2041
Marshall stability (kN)	10.1	ASTM D-6927 – 15
Marshall flow (mm)	2.8	ASTM D-6927 – 15
Specific gravity at optimum asphalt content	2.290	ASTM D-1188
Volume of voids (%)	4.9	ASTM D-2041
Voids filled with asphalt binder (%)	78	ASTM D-2041

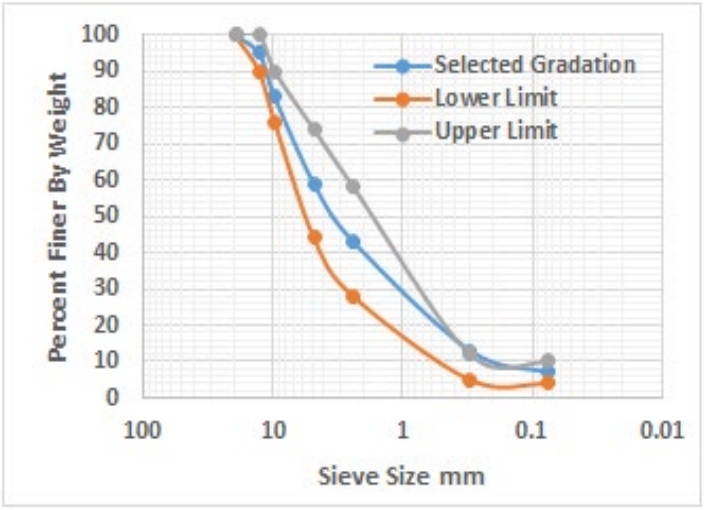

Figure 1. Combined gradation of asphalt concrete

2.5. Preparation and testing of asphalt concrete specimens

Asphalt concrete specimens of 152.4 mm diameter and 38.1 mm thickness were constructed using the traditional CBR mold and spacers, the required amount of hot Asphalt concrete mix (at 160 ˚ C) which gives the predetermined density of (2.290 gm / cm^3) at optimum asphalt content

of 4.8 % was weighted, spread into the preheated mold, and subjected to initial compaction through a 50 spatula strikes, then the specimens were subjected to static compaction using Versa compression machine until the required specimen thickness was obtained at the target density, a total load of 5000 kg was required. The specimens were compacted to 95 % of the maximum theoretical density. Filter papers have been introduced at the top and bottom faces of the specimens to prevent sticking to the spacers. Specimens were kept overnight to cool then withdrawn from the mold using hydraulic jack. For control specimens, the material required to construct the upper layer which represent the overlay (when it was loose at 160 ^{0} C) was compacted over the pre compacted lower layer specimen which represent the existing pavement layer, this could simulate the field condition when constructing an overlay over existing pavement layer. The bonding between the upper and lower specimens is expected to occur due to the high compaction temperature rather than the need for a tack coat. However, for reinforced system, the material required to construct the upper layer (overlay) (when it was loose at 160 ^{0} C) was compacted over the pre compacted lower layer specimen after inserting the geogrid in between. The expected bonding between the upper and lower specimens and the geogrid occurs due to the high compaction temperature of 160 ^{0} C and interlock of aggregates with the geogrid rather than the need for a tack coat. The coupled specimens (upper and lower) were seated into the testing box model of 50 x50 x70 cm dimensions on a layer of loose sand of 40 cm depth. The loose sand condition has been selected so that it could simulate compressible and poor subgrade, so that the reinforcing effect of asphalt concrete could be clearly detected. The loose sand was added into the model box by raining method. It was poured from height not exceeding 20 cm in layers, 100 mm for each layer until the desired height of sand was reached, and the layer was leveled with a straight edge. The sand is classified as poorly graded sand with a coefficient of uniformity (C_u)= 1.57 and coefficient of curvature (C_C) = 1. The maximum and minimum dry unit weight of sand are 17.4 kN/m^3 and 14.7kN/m^3 respectively and the specific gravity value of the used sand is 2.65.

The load was applied through a circular metal plate of 10 mm thickness and 40 mm diameter using a strain-controlled system. An initial seating load of 10 Newton was applied consistently for all the tested specimens to ensure perfect contact between the plate and asphalt concrete top surface, also such contact was insured between the loose sand and the bottom face of Asphalt concrete. The thickness of the overlay specimens and the size of the loading plate were modelled to represent 50 % of the real field size (60 mm is the typical overlay thickness and 80 mm is the tire print). The load was applied to exhibit punching shear type of failure and maintained at a rate of 2 mm / minutes and the load – deformation data were recorded until failure. The adopted failure criteria of asphalt concrete specimens were the drop in load among increasing the deformation and the punching deformation which is monitored by visual observation using bubble level. A total of 12 asphalt concrete specimens have been constructed and tested in duplicate. Figure 2 exhibits the preparation, compaction, and the check of deformation of asphalt concrete cylindrical specimens with the aid of CBR molds and spacers. The accepted standard deviation between the strength and deformation values of each couple of specimens was 5 % and the average value of a minimum duplicate specimens was considered for the analysis for each testing condition.

Figure 2. Preparation and compaction of asphalt concrete specimens with the aid of CBR molds and spacers

Figure 3 shows the preparation of grid reinforced specimens with various types of reinforcements. The compaction temperature was maintained to 160 ˚C. The 50-Ton capacity compression machine was used for static compaction of the specimens and for testing the coupled specimens in the model box.

Figure 3. Preparation and testing of geogrid reinforced asphalt concrete samples

3. Results and Discussion

3.1. Influence of geogrids on load bearing and deformation

Figure 4 exhibits the load-deformation characteristics of control and geogrid reinforced asphalt concrete. It can be observed that there is a significant increase in the load sustaining capacity of asphalt concrete after the implication of geogrid reinforcement as compared with the control mixture.

The trend of the load-deformation was sharp at early stage of practicing the stress for reinforced mixtures, while it changes to gentle after a punching deformation of 10 mm regardless of the geogrid type. However, the trend of increment in the load-deformation for control mixture (unreinforced) changes from sharp to gentle after 3 mm of punching deformation. This may be attributed to the ability of geogrids to increase the load bearing capacity of asphalt concrete due to generated particle interlock by the aperture of the geogrids. Smaller aperture size and lower thickness of geogrid had furnished higher load bearing capacity of 2.5 kN for Tensar AR-1 geogrid as compared with that of 2.49 kN provided by Tensar AR-G geogrid. This may be attributed to a more homogeneous mixture obtained by the small aperture size and low rib thickness within the limited thickness of the overlay layer nominal particle size of aggregates. On the other hand, at failure, both geogrids type exhibit higher load bearing capacity of (56.25 and 55.62) % for (Biaxial 0.8 and Biaxial 1.2) respectively. Similar behavior was reported by Correia and Zornberg, 2016 [5]; Zarei et al., 2025 [12].

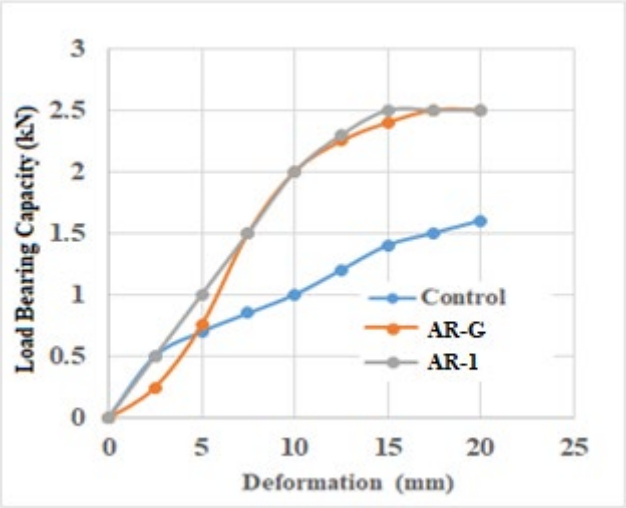

Figure 4. Influence of geogrids of load bearing capacity of asphalt concrete

3.2. Influence of geogrids on failure stages of asphalt concrete

The control asphalt concrete specimen exhibited changes in the failure stage from viscoelastic to viscoplastic after 2.5 mm of punching deformation. However, when the geogrids were implicated, a significant variation in the failure mechanism could be detected. The change of failure stage from viscoelastic to viscoplastic appeared after 10 mm of punching deformation which was checked with the aid of bubble level. This could be attributed to the restriction of lateral creep of asphalt concrete mixture under the applied punching stress due to the particle interlock offered by the geogrids. Such behavior agrees with the findings reported by Bekheet et al, 2019 [21]. Figure 5 demonstrates the graphical representation of failure stages of control and reinforced asphalt concrete.

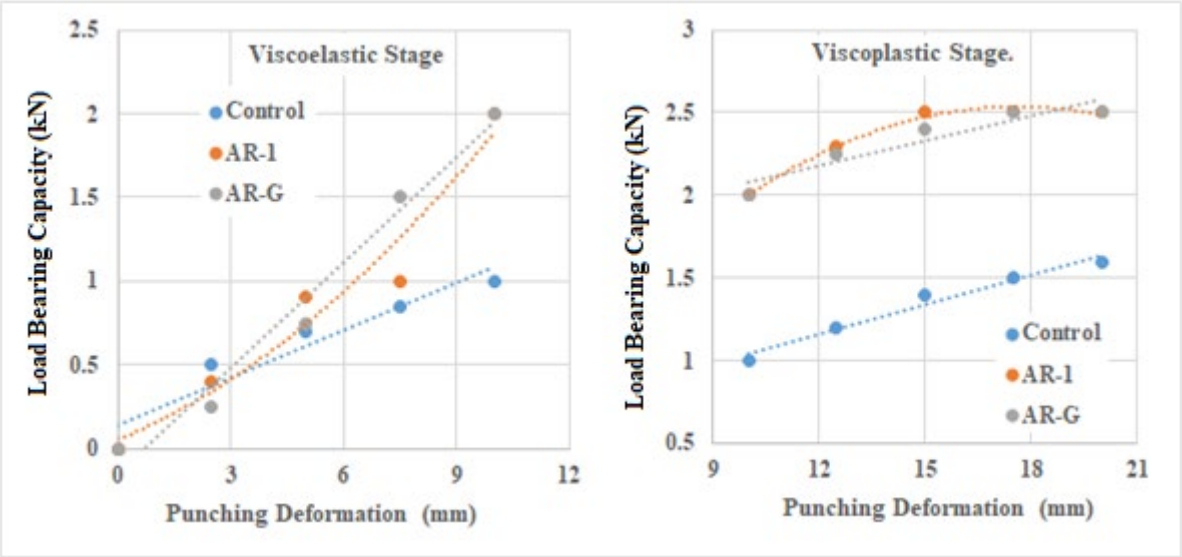

Figure 5. Graphical representation of failure stages

Table 5 summarizes the influence of geogrids on the viscoelastic behavior of asphalt concrete. It can be observed that during the viscoelastic and viscoplastic stage of failure, the control mixture exhibits a gentle and linear trend of failure due to the homogeneity of the asphalt concrete mixture. When the geogrids were introduced as an interlayer to asphalt concrete, the failure trend changed to polynomial mode with high coefficients of determination for AR-1 geogrid. On the other hand, the implication of AR-G geogrid exhibits a linear mode of failure through both stages. Similar findings were reported by Kumar and Jallu, 2022 [20]. The choice of linear or polynomial models was based on the high coefficient of determination (R^2) provided by each and the observed scatter of data.

Table 5. Mathematical models of failure stages

Geogrid type	Failure stages			
	Viscoelastic stage Mathematical model R^2		Viscoplastic stage Mathematical model R^2	
Control	Y= 0.094 X + 0.14	0.917	Y= 0.06 X + 0.44	0.969
Biaxial 0.8, AR-1	Y= 0.009 X^2 + 0.0926 X +0.0543	0.951	Y= - 0.009 X^2 +0.322 X +0.302	0.988
Biaxial 1.2, AR-G	Y= 0.21 X – 0.15	0.975	Y= 0.05 X + 1.58	0.877

3.3. Influence of geogrids on stiffness of asphalt concrete

Figure 6 exhibits the influence of geogrids on the stiffness of asphalt concrete. It can be detected that the implementation of geogrids exhibited higher stiffness of asphalt concrete as compared with that of the control mixture. This may be attributed to the interlocking of aggregate particles with the ribs and aperture of the geogrids. At failure, the stiffness of the grid reinforced asphalt concrete is higher than that of the control mixture by (56.2, and 62.5) % for AR-1 and AR-G geogrids respectively. It can be revealed that implementation of geogrids has changed the properties of asphalt concrete from flexible to semi-rigid as exhibited in Figure 6.

Such findings from the implemented testing program could be beneficial in the decision for overlay and the future requirements from such rehabilitation regarding the sustainability issue and the cost effectiveness.

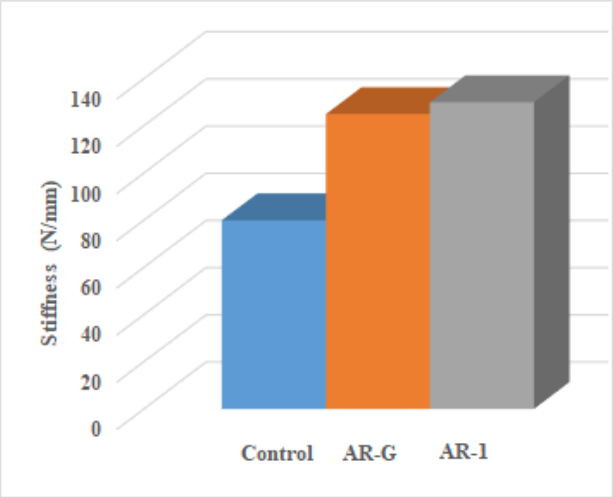

Figure 6. Influence of geogrid on the stiffness of asphalt concrete

4. Conclusions

Based on the limited testing program and limitations of materials, the following remarks may be addressed:

- Smaller aperture size and lower thickness of geogrid had furnished higher load bearing capacity of 2.5 kN for Tensar AR-1 biaxial 0.8 geogrid as compared with that of 2.49 kN provided by Tensar AR-G biaxial 1.2 geogrid.
- At failure, both geogrids type exhibit higher load bearing capacity of (56.25 and 55.62) % for (Biaxial 0.8 and Biaxial 1.2) respectively.
- When the geogrids were implicated, a significant variation in the failure mechanism could be detected. The change of failure stage from viscoelastic to viscoplastic appeared after 10 mm of punching deformation.
- When the geogrids were introduced as an interlayer to asphalt concrete, the failure trend changed to polynomial mode with high coefficients of determination for AR-1 geogrid. On the other hand, the implication of AR-G geogrid exhibits a linear mode of failure through both stages.
- At failure, the stiffness of the grid reinforced asphalt concrete is higher than that of the control mixture by (56.2, and 62.5) % for AR-G and AR-1 geogrids respectively.
- Geogrids are recommended to improve the load bearing capacity of asphalt concrete.
- Various overlay thickness, loading rate, testing environment, and geogrid type are recommended for future testing programs.

Declaration of Conflict of Interests

The author declares that there is no conflict of interest. They have no known competing financial interests or personal relationships that could have appeared to influence the work reported in this paper.

References

[1.] Zofka A., Maliszewski M., Zofka E., Paliukaitė M., Žalimienė L. Geogrid reinforcement of asphalt pavements. The Baltic journal of road and bridge engineering. 2017 Volume 12(3): P. 181–186. http://doi:10.3846/bjrbe.2017.22

[2.] Brusa, N.; Crowther, D.; Pezzano, P. Asphalt reinforcement through geosynthetics: design method and UK experience. In Proceedings of the LJMU 15th Annual International Conference on Asphalt Pavement Engineering and Infrastructure, 24–25 February 2016, Liverpool, UK. Vol. 15. https://1stdirectory.co.uk

[3.] Zofka, A., Maliszewski, M., & Maliszewska, D. Glass and carbon geogrid reinforcement of asphalt mixtures. Road Materials and Pavement Design, 18 issue (sup1), 2017. Taylor and Francis, Road Materials and Pavement Design. Papers from the 91st Association of Asphalt Paving Technologists' Annual Meeting P. 471–490. https://doi.org/10.1080/14680629.2016.1266775

[4.] Correia N., and Zornberg j. Mechanical response of flexible pavements enhanced with geogrid-reinforced asphalt overlays. MDPI Geosynthetics International, 23, No.3, 2016. P. 183–193. http://dx.doi.org/10.1680/jgein.15.00041

[5.] Correia N., and Zornberg j. Strain distribution along geogrid-reinforced asphalt overlays under traffic loading. Elsevier Geotextiles and Geomembranes, Volume 46, Issue 1, February 2018, P. 111-120. https://doi.org/10.1016/j.geotexmem.2017.10.002

[6.] Lee S., Phan T., Park D. Evaluation of carbon grid reinforcement in asphalt pavement. Elsevier Construction and Building Materials. Volume 351, 10 October 2022, 128954. https://doi.org/10.1016/j.conbuildmat.2022.128954

[7.] Orešković, M., Bohuš, Š., Virgili, A., Canestrari S. Simplified methodology for fatigue analysis of reinforced asphalt systems. Springer Nature Mater Struct 57, 34, 2024. https://doi.org/10.1617/s11527-024-02305-1

[8.] Alimohammadi H., Zheng J., Schaefer V., Siekmeier J., Velasquez R. Evaluation of geogrid reinforcement of flexible pavement performance: A review of large-scale laboratory studies. Elsevier Transportation Geotechnics, Volume 27, 2021, 100471, https://doi.org/10.1016/j.trgeo.2020.100471

[9.] Mounes S., Karim M., Khodaii A., Almasi M. Evaluation of permanent deformation of geogrid reinforced asphalt concrete using dynamic creep test. Elsevier Geotextiles and Geomembranes, 44 (1). 2016. https://doi.10.1016/j.geotexmem.2015.06.003

[10.] Correia N., and Mugayar A. Effect of binder rates and geogrid characteristics on the shear bond strength of reinforced asphalt interfaces. Elsevier Construction and Building Materials 269(121292): 2021. P.1-11. https://doi:10.1016/j.conbuildmat.2020.121292

[11.] Ziegler M. Application of Geogrid Reinforced Constructions: History, Recent and Future Developments. Elsevier Procedia Engineering. Volume 172, 2017, P. 42-51 https://doi.org/10.1016/j.proeng.2017.02.015

[12.] Zarei S., Wang W., Ouyang J., Liu W. Failure mechanisms of geogrid-reinforced asphalt pavements: A viscoelastic 3D FEM analysis. Elsevier Construction and Building Materials, Volume 476, 2025, 141217, https://doi.org/10.1016/j.conbuildmat.2025.141217

[13.] Solatiyan E., Bueche N., Carter A. Laboratory evaluation of interfacial mechanical properties in geogrid-reinforced bituminous layers. Elsevier Geotextiles and Geomembranes, Volume 49, Issue 4, 2021. P. 895-909. https://doi.org/10.1016/j.geotexmem.2020.12.014

[14.] Liu Z., Xue J., Xiao J., Kong Q. Behaviors of geogrid-reinforced asphalt pavement over a localized void under cyclic loading. Elsevier Transportation Geotechnics, Volume 46, 2024, 101238, https://doi.org/10.1016/j.trgeo.2024.101238

[15.] Chango I., Cyriaque A., Yan M., Xianzhang L., Mitobaba J. Impact Assessment of Asphalt Concrete in Geogrid-Reinforced-Pile-Supported Embankment During High-Speed Train Traffic. The Baltic Journal of Road and Bridge Engineering, 17(2) P. 135-163. January 2022. https://doi:10.7250/bjrbe.2022-17.563

[16.] Nguyen T., Toledo K., and Huynh T. Assessing reinforced pavement performance: Influence of geogrid position, axial stiffness, and applied stress. CTU Journal of Innovation and Sustainable Development Vol. 16, Special Issue: ICCEE (2024): P. 28-34. https://doi:10.22144/ctujoisd.2024.278

[17.] Sarsam S. Deformation Characteristics of Textile and Grid Reinforced Asphalt Concrete Pavement Model. Sciknow Publications Ltd. RAM (2013), 1(5): P. 49-55. Research and Application of Material https://www.researchgate.net/publication/275570646

[18.] Graziani A., Pasquini E., Ferrotti G., Virgili A., Canestrari F. Structural response of grid-reinforced bituminous pavements. Springer Nature, Materials and Structures Volume 47, p. 1391–1408· January 2014. https://doi.org/10.1617/s11527-014-0255-1

[19.] Reinforced with Geocomposite. Ragni D., Montillo T., Marradi A., Canestrari F. Fast Falling Weight Accelerated Pavement Testing and Laboratory Analysis of Asphalt Pavements. Springer Nature Switzerland AG 2020 Book chapter: ISAP APE, LNCE 48, P. 417–430, 2020. https://doi.org/10.1007/978-3-030-29779-4_41

[20.] Kumar R., and Jallu H. Performance of Geogrid Reinforced Asphalt Layers—A Review. Springer Nature Singapore Pte Ltd. 2022, Recent Advancements in Civil Engineering, Lecture Notes in Civil Engineering 172, P. 683-699, https://doi.org/10.1007/978-981-16-4396-5_60

[21.] Bekheet W., Rowan A., Moussa G. Reinforcement of asphalt concrete layers using biaxial and triaxial geogrids. Conference: The tenth Alexandria international conference on structural, geotechnical engineering and management "AICSGE-10". December 2019.

[22.] Leiva-Padilla, P., Loria-Salazar, L., Aguiar-Moya, J., Leiva-Villacorta, F. Reflective Cracking in Asphalt Overlays Reinforced with Geotextiles. 8th RILEM International Conference on Mechanisms of Cracking and Debonding in Pavements. RILEM Book series, vol 13. 2016. Springer, Dordrecht. https://doi.org/10.1007/978-94-024-0867-6_31

[23.] Alimohammadi H., Schaefer V., Zheng J., White D., Zheng G. A State-of-the-art Large-scale Laboratory Approach to Evaluating the Effectiveness of Geogrid Reinforcement in Flexible Pavements. Geosynthetics Conference February 2021. Industrial Fabrics Association International. P. 618-628. https://www.researchgate.net/publication/351512596

[24.] Canestrari, F. D'Andrea A., Ferrotti G., Graziani A., Partl M., Petit C., Raab C., Sangiorgi C. Advanced Interface Testing of Grids in Asphalt Pavements. Testing and Characterization of Sustainable Innovative Bituminous Materials and Systems. RILEM State-of-the-Art Reports, vol 24. Springer, Cham. 2018. https://doi.org/10.1007/978-3-319-71023-5_4

[25.] ASTM. Road and Paving Materials, Annual Book of ASTM Standards, Volume 04.03, American Society for Testing and Materials. West Conshohocken, USA. (2015). www.astm.com

[26.] SCRB. State Commission of Roads and Bridges. Standard Specification for Roads & Bridges, R-9 Asphalt concrete. Ministry of Housing & Construction, Baghdad-Iraq. (2003).

How to Cite This Article

Sarsam, S.I., Behavior of Plastic-Geogrid Reinforced Asphalt Concrete, Civil Engineering Beyond Limits, 3(2025), 11005. https://doi.org/10.36937/cebel.2025.11005